EFFECT OF PILOT TONE-BASED MODULATOR BIAS CONTROL ON EXTERNAL MODULATION LINK PERFORMANCE

Edward I. Ackerman and Charles H. Cox III
Photonic Systems, Inc.
100 Wildwood Dr., Carlisle, Massachusetts 01741
Phone: (978) 369-0729, FAX: (978) 318-0556, email: eackerman@photonicsinc.com

ABSTRACT

The dynamic range of an external modulation link in which a pilot tone maintains a Mach-Zehnder modulator at quadrature bias is limited to $64/(\pi\, m_{PT})^4$, where m_{PT} is the modulation depth of the pilot tone.

INTRODUCTION

In an analog external modulation link that uses an external modulator, the third-order intermodulation distortion products generated by the modulator's nonlinear transfer function set the upper limit on the RF signal powers that can be relayed by the link with high signal fidelity. If the laser that provides unmodulated light to the modulator has sufficiently low relative intensity noise (RIN), then shot noise sets the lower limit on the RF signal power.

Analytical models [1] and experimental measurements [2] have both shown that, for an external modulation link that uses a Mach-Zehnder interferometric modulator (MZM) at its quadrature bias and a detector operating at a DC photocurrent of 2.5 mA, the range of RF signal powers between these two limits, which is the intermodulation-free dynamic range ($IMFDR_3$), is approximately 110 dB · $\mathrm{Hz}^{2/3}$. In this paper we show that the conventional method of maintaining the MZM bias at quadrature, involving the injection of a pilot tone with a typical modulation depth of 2.5%, reduces this $IMFDR_3$ to roughly 62 dB.

ANALYSIS

The bold curve in Figure 1 shows the transfer function of an MZM, which dictates how the link's output RF signal power and second-order distortion products vary with modulator bias. Maintaining the MZM bias at quadrature is especially important in links operating in systems with bandwidths wider than one octave, because only at the quadrature bias point are second-order distortion products minimized.

Figure 2 shows the method that is used most frequently for maintaining MZM bias voltage at quadrature point. This consists of a local oscillator that generates a pilot tone, usually at around 1 kHz or so, and a photodetector that taps a small percentage of the MZM's optical output power. The photodetector feeds a circuit that filters out all but the second harmonic of the pilot tone frequency, and a feedback loop continuously adjusts the MZM's DC bias voltage to minimize the detected second harmonic.

Injecting a pilot tone to control the MZM's bias point lowers the link's $IMFDR_3$ because the third-order nonlinearity of the modulator's transfer function results in intermodulation distortion products at two ***in-band*** frequencies equal to the desired RF signal frequency plus and minus twice the pilot tone frequency. These distortion products appear at the link output and cannot be filtered out unless one limits the link's operational bandwidth to less than twice the pilot tone frequency.

For the external modulation link in Figure 2, in which a quadrature-biased MZM is modulated by two-tone signal $v_{RF}\left(\cos\omega_{RF1}t+\cos\omega_{RF2}t\right)$ and pilot tone $v_{PT}\cos\omega_{PT}t$, the optical power illuminating the detector, P_D, can be represented as:

$$P_D = P_{D,\max}\left[\frac{1}{2}+\frac{\pi}{2}\left[m_{RF}\left(\cos\omega_{RF1}t+\cos\omega_{RF2}t\right) + m_{PT}\cos\omega_{PT}t\right]+\frac{\pi^3}{12}\left[m_{RF}\left(\cos\omega_{RF1}t + \cos\omega_{RF2}t\right)+m_{PT}\cos\omega_{PT}t\right]^3 + \mathrm{K}\right], \quad (1)$$

where $P_{D,\max}$ is the optical power illuminating the photodetector at the output of the link when the MZM is biased for maximum transmission, and where the modulation depth m is defined as v/V_π. Expressing P_D as a function of m allows for the possibility that the RF and pilot tones are applied to separate electrodes of the MZM, which may have different V_π's.

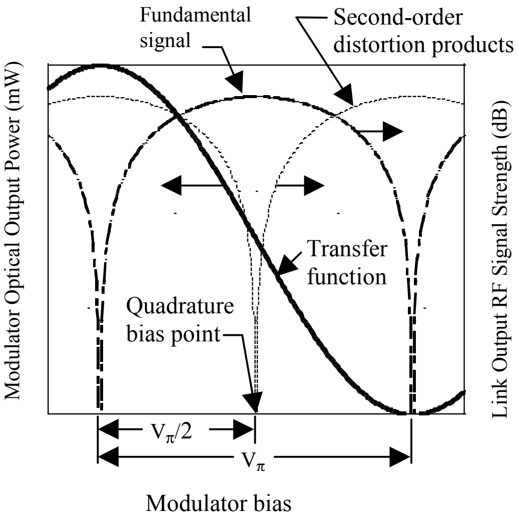

Fig. 1 Transfer function of an MZM, plus the link output power at the fundamental RF and second-order distortion frequencies.

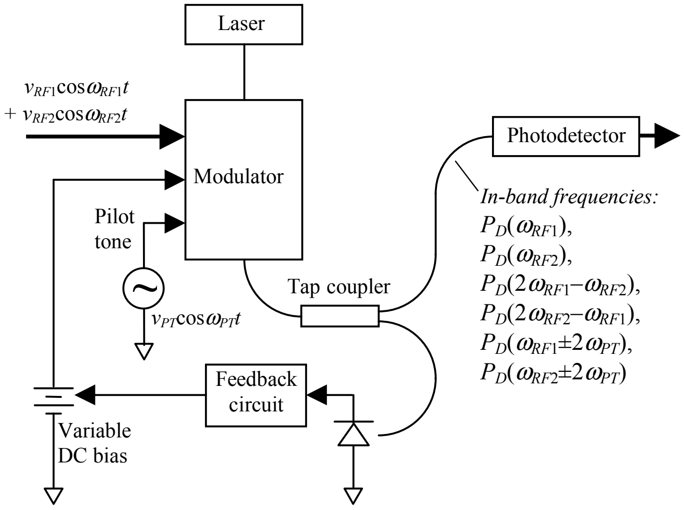

Fig. 2 Method of controlling external modulator bias by injecting a pilot tone and using feedback correction to maintain quadrature bias.

To determine the effect of the pilot tone on the link's dynamic range requires using equation (1) to calculate the magnitude of P_D at three frequencies: 1) RF signal frequency ω_{RF1} (or equivalently, ω_{RF2}), 2) in-band intermodulation distortion product frequency $2\omega_{RF1}-\omega_{RF2}$ (or equivalently, $2\omega_{RF2}-\omega_{RF1}$), and 3) in-band intermodulation frequency $\omega_{RF1} \pm 2\,\omega_{PT}$ (or equivalently, $\omega_{RF2} \pm 2\,\omega_{PT}$):

$$\left|P_D\left(\omega_{RF1}\right)\right| = P_{D,\max}\,\frac{\pi}{2}\,m_{RF}\,; \tag{2}$$

$$\left|P_D\left(2\omega_{RF1}-\omega_{RF2}\right)\right| = P_{D,\max}\,\frac{\pi^3}{16}\,m_{RF}^3\,; \tag{3}$$

$$\left|P_D\left(\omega_{RF1}\pm 2\omega_{PT}\right)\right| = P_{D,\max}\,\frac{\pi^3}{16}\,m_{RF}\,m_{PT}^2\,. \tag{4}$$

The photodetector at the link output generates electrical power at each of these frequencies according to the relation:

$$P_{out} = \frac{1}{2}\left|I_D\right|^2 R_{out}\,, \tag{5}$$

where I_D is related to P_D through the detector responsivity, and where R_{out} is the link output impedance. The detector also generates shot noise power at the link output as follows:

$$\begin{aligned} N_{out} &= 2q\left\langle I_D\right\rangle R_{out}B \\ &= q\,I_{D,\max}R_{out}B \text{ at quadrature bias,} \end{aligned} \tag{6}$$

where q is the electronic charge and B is the instantaneous receiver bandwidth.

For a link that sees two equal-power input RF signal tones, Figure 3 shows how the link output powers at the three frequencies in equations (2)-(4) vary with input power. Also plotted in Figure 3 is the link output noise power, which is independent of the RF input power and which is assumed to be dominated by the shot noise. In the absence of a pilot tone, shot noise limits $IMFDR_3$ of an MZM-based external modulation link to a value of:

$$IMFDR_3 = \left(\frac{I_{D,\max}}{q\,B}\right)^{2/3}, \tag{7}$$

which corresponds to about 110 dB · $\mathrm{Hz}^{2/3}$ for $\left\langle I_D\right\rangle = I_{D,\max}/2 = 2.5\,\mathrm{mA}$. In addition Figure 3 shows that, when a pilot tone is present, $IMFDR_3$ can be limited by the mixing of an RF tone and the pilot tone rather than by the mixing of two RF tones. Thus the actual link dynamic range is whichever is smaller of what was calculated using equation (7) or

$$IMFDR_3 = \frac{64}{\left(\pi\,m_{PT}\right)^4}\,. \tag{8}$$

Note that Equation (8), which is simply the square of the ratio of equations (2) and (4), depends only on the pilot tone strength and not on B.

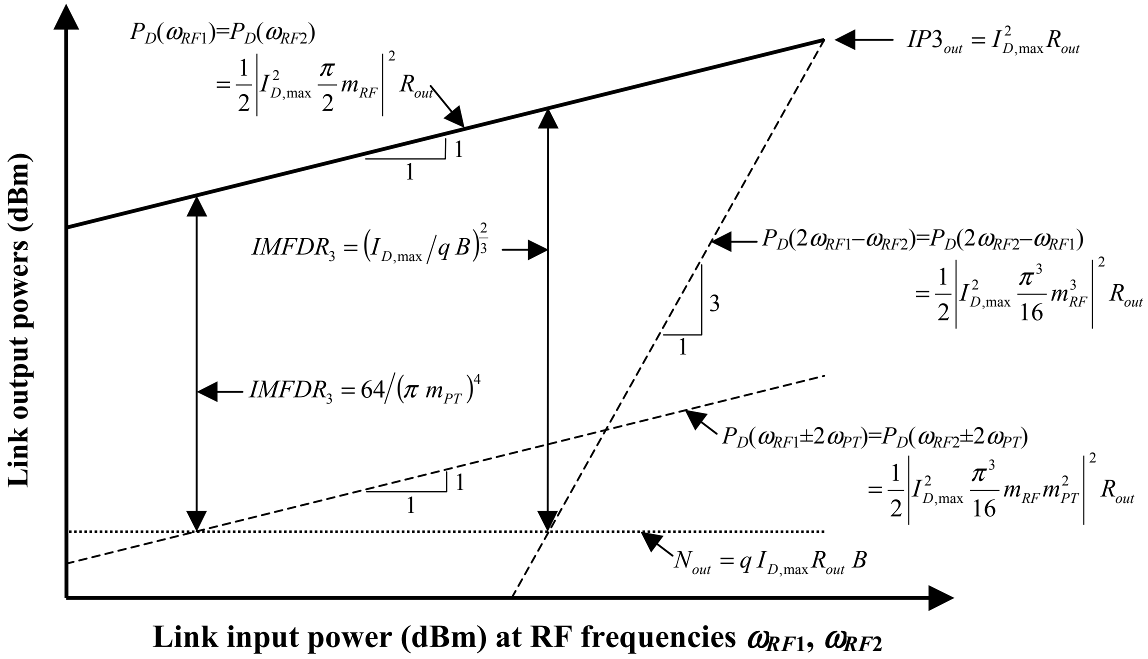

Fig. 3 Relationship between MZM-based external modulation link's two-tone input signal power and output powers at the tone frequencies and at the frequencies where in-band distortion products are generated. Like the output power at the signal frequencies ω_{RF1} and ω_{RF2}, the output powers at the in-band intermodulation distortion frequencies $\omega_{RF2}\pm 2\ \omega_{PT}$ and $\omega_{RF2}\pm 2\ \omega_{PT}$ increase linearly (*i.e.,* with a slope of 1) with respect to link input power at ω_{RF1} and ω_{RF2}. Thus, as the figure shows, the degree of $IMFDR_3$ degradation caused by the use of the pilot tone depends on the receiver instantaneous bandwidth B.

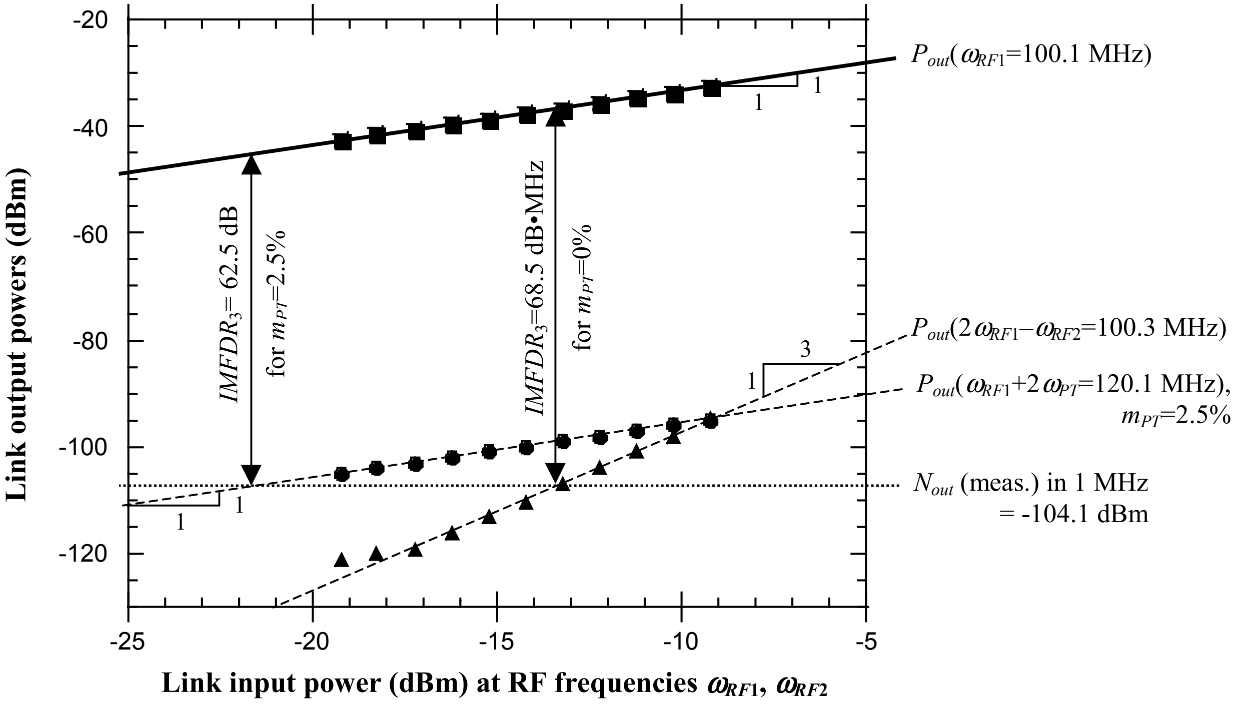

Fig. 4 Results of two-tone intermodulation distortion measurement on an MZM-based external modulation link with and without pilot-tone based modulator bias control (*i.e.*, with pilot tone modulation depth m_{PT}=2.5% and 0%, respectively). Measured data and extrapolated curves are shown.

EXPERIMENT

To verify that Figure 3 and the equations from which it is derived are valid, we performed measurements on the type of link diagrammed in Figure 2. We used an InGaAsP diode laser with a PM fiber pigtail to provide 30 mW of low-RIN optical power at λ=1.55 µm to the modulator. For the modulator we used a standard lithium-niobate MZM with an input PM fiber and output SM fiber pigtail and with separate RF and DC bias electrodes. The DC electrode exhibited a V_π of about 4.8 V. For the signal photodetector we used an InGaAs PIN photodiode with a responsivity of 0.9 A/W. The laser bias current was adjusted such that when the MZM was at quadrature bias we measured 2.5 mA of DC photocurrent.

For the experiment we used two signal generators to provide the modulator's RF input port with tones at 99.9 MHz and 100.1 MHz, and used an RF spectrum analyzer with the resolution bandwidth set to B=1 MHz to measure link output signal and noise powers at all frequencies of interest. We performed two-tone intermodulation distortion measurements with the MZM bias controlled manually, and subsequently with a 10 MHz pilot tone of amplitude v_{PT}=120 mV (=2.5% of 4.8 V) applied to the DC electrode of the MZM. The individual data points on the plot in Figure 4 show how our measurements confirmed that, for these values of B and m_{PT}, $IMFDR_3$ is degraded by about 6 dB due to the use of a pilot tone-based MZM bias controller. Note that for smaller values of B, the output noise would be proportionally smaller, and therefore the $IMFDR_3$ degradation due to the pilot tone would be even more pronounced.

CONCLUSIONS

We have shown that using a pilot tone-based control circuit to maintain a modulator's optimum bias point can have a detrimental effect on an external modulation link's dynamic range. The specific extent of the performance degradation depends on the instantaneous bandwidth of the receiver in the system, and on the strength of the pilot tone.

To counteract this effect, a bias control circuit of this type may need to use a weaker pilot tone in conjunction with an optical coupler that has a higher tap percentage. For instance, reducing the typical pilot tone modulation depth from 2.5% to 0.5% implies that the typical 1% optical tap coupler should be replaced by a 5% coupler in order to maintain the same detection sensitivity.

The findings we have reported and experimentally verified using an MZM also carry implications for other types of external modulators—including "linearized" modulators, in which the third-order distortion is cancelled using one of a variety of methods [3]. That is, if the linearized bias point is maintained using a pilot tone-based feedback circuit, the modulator may generate stronger in-band intermodulation distortion products by mixing the pilot tone with an input RF tone than by mixing two input RF tones, resulting in smaller link dynamic range than what the linearized modulator would otherwise enable.

REFERENCES

[1] E. Ackerman and C. Cox, "Trade-offs between the noise figure and dynamic range of an analog optical link," *Proc. Photonic Systems for Antenna Applications Conf.*, February 2000.

[2] G. Betts, C. Cox, and K. Ray, "20-GHz optical analog link using an external modulator," *IEEE Photon. Technol. Lett.*, vol. 2, pp. 923-925, December 1990.

[3] U. Cummings and W. Bridges, "Bandwidth of linearized electro-optic modulators," *J. Lightwave Technol.*, vol. 16, pp. 1482-1490, August 1998.